

Flat branches and pressure amorphization

Morrel H. Cohen, Jorge Íñiguez, and J. B. Neaton

Department of Physics and Astronomy, Rutgers University, Piscataway, New Jersey 08854-8019, USA

After summarizing the phenomenology of pressure amorphization (PA), we present a theory of PA based on the notion that one or more branches of the phonon spectrum soften and flatten with increasing pressure. The theory expresses the anharmonic dynamics of the flat branches in terms of local modes, represented by lattice Wannier functions, which are in turn used to construct an effective Hamiltonian. When the low-pressure structure becomes metastable with respect to the high-pressure equilibrium phase and the relevant branches are sufficiently flat, transformation into an amorphous phase is shown to be kinetically favored because of the exponentially large number of both amorphous phases and reaction pathways. In effect, the critical-size nucleus for the first-order phase transition is found to be reduced to a single unit cell, or nearly so. Random nucleation into symmetrically equivalent local configurations characteristic of the high-pressure structure is then shown to overwhelm any possible domain growth, and an “amorphous” structure results.

I. INTRODUCTION

Since its first observation in $\text{Gd}_2(\text{M}_2\text{O}_4)$ in 1972,¹ and especially in ice nearly twenty years ago,² amorphization induced by pressure (or “pressure amorphization”, PA) has been discovered in materials of essentially all binding types, from ionic to metallic, which have more than one atom per primitive cell. The disappearance of the X-ray diffraction pattern of the low-pressure crystalline phase, or a concomitant broadening of peaks in the vibrational spectra, is taken to be evidence of an emerging amorphous state. These signatures typically appear within a pressure window whose average value and overall range are strongly material dependent.

The phenomenology and simulations of materials displaying pressure amorphization have been thoroughly reviewed.^{3,4,5,6,7} It is not sufficiently generally recognized within that extensive literature that there are two distinct classes of materials which could be labelled as pressure amorphized. In the first, a conventional glass, the atomic structure is not topologically equivalent to any crystalline structure. In the second, random displacements of the nuclei occur which do not destroy crystalline topology.

Despite extensive investigation, and in part because the above distinction has not been clearly made, a general physical picture of the microscopic processes underlying PA has yet to emerge. On the theoretical side, the main efforts have focused on two materials exhibiting the second class of PA, $\alpha\text{-SiO}_2$ ($\alpha\text{-quartz}$)^{8,9,10,11,12,13,14,15,16,17} and $\alpha\text{-AlPO}_4$.^{10,13,18,19} Both interatomic potentials and fully first-principles approaches have been used to study these systems. While it remains uncertain whether PA has been actually observed in a simulation, it seems to be generally accepted that there is a correlation between pressure amorphization and the softening (i.e., phonon frequencies approaching zero) of a nearly dispersionless, or flat, acoustic phonon branch. In addition, it has been suggested that the occurrence of an amorphous phase should be strongly related to the dynamics of the system.^{10,17}

In this paper, we discuss an explicit model for materials exhibiting the second class of PA. On the basis of inferences drawn from both phenomenology and simulations, we first argue that these materials share many common features and then show how to construct an effective Hamiltonian that incorporates these features. As we demonstrate, this microscopic model is simple enough to analyze in detail yet still relevant to real materials.

The paper is organized as follows. In Section II we discuss the elements of our theory of PA on the basis of both phenomenology and simulations. In Section III we review some elements of lattice vibration theory. In Section IV, we present an effective Hamiltonian suitable for the discussion of the physics underlying PA, and reduce it to the simplest model capable of incorporating the essential features discussed in Section II. In Section V, we describe how PA is manifested in the simple model through an analysis of the topology of the model’s potential energy surfaces. Sections VI, VII, and VIII address the conditions for the occurrence of pressure amorphization in the 2-site, 3-site, and N -site models respectively. In Section IX, we discuss the relation of our considerations to conventional nucleation and growth models of structural transitions. We summarize our results and draw conclusions in Section X.

II. PHENOMENOLOGY AND SIMULATIONS

Many transition patterns have been observed during pressure amorphization.^{3,5,6} Of these, we select five (types I-V) for explicit discussion:

Type I materials transform from a crystalline phase C to an amorphous phase a at pressure $p = p_{ca}$. Then, after p is reduced from above p_{ca} , they remain amorphous down to a lower pressure p_{ac} , below which they revert to C , as is the case, for example, in AlPO_4 .¹⁸ (The hysteresis $p_{ca}-p_{ac}$ is large, typically of the order of p_{ca} itself.) Materials of type II remain amorphous upon release of pressure, making possible detailed examination of the properties of the amorphous phase. This appears to be the case for amorphous $\alpha\text{-SiO}_2$, which has been found to

retain elastic anisotropy.^{20,21} Another example is crystalline Fe₂SiO₄-fayalite, which is antiferromagnetic; the pressure-amorphized fayalite remains antiferromagnetic with the Neel temperature essentially unchanged,^{22,23,24} from which we infer that the *a*- and *C*-phase topologies are the same. Type III materials become amorphous above p_{ca} , later transforming to a new crystal structure *C'* when *p* is held steady above p_{ca} for sufficiently long. Materials of type IV behave the same as those of type I as *p* is reduced from above p_{ca} , but they transform to a new crystal structure *C'* from the amorphous phase *a* when pressure is increased beyond $p_{ac'} > p_{ca}$. Finally, materials of type V transform to *C'* at $p_{ac'}$ upon decompression from above p_{ac} , finally reverting to *C* below $p_{cc'}$.

As already mentioned in the Introduction, lattice dynamical calculations have shown a considerable softening of the entire lowest band of α -quartz, with a soft mode instability occurring first at the zone boundary at pressures at which PA is observed^{12,16} or at somewhat higher pressures.¹⁵ Also, it has been argued that the transition mechanism in α -AlPO₄ is similar to that of α -quartz.^{10,19}

From the phenomenology and calculations described above, the following picture of PA emerges: The random displacements in the amorphous phase are associated with the incipient instability of at least one nearly flat phonon branch. The amorphous phase is the result of a kinetically hindered transition between two closely-related crystalline phases *C* and *C'*, where *C* is a low-pressure crystalline phase and *C'* is a high-pressure one. The transition from *C* to *C'* is expected to be strongly first order, and also displacive, meaning that the atomic structure of *a* remains topologically equivalent to that of *C*. (This latter feature is to be contrasted with the significant changes in topology that usually accompany ordinary glass formation.) In the amorphous phase *a*, random displacements are large enough to eliminate the diffraction pattern through reduction of the Debye-Waller factor, but not so large so as to disrupt the topology of the crystal structure associated with *C*.

III. NEARLY FLAT BRANCHES; LOCAL MODES AS LATTICE WANNIER FUNCTIONS

Let us assume that we can work in the Born-Oppenheimer approximation, suppressing all the electronic degrees of freedom. The Hamiltonian is, then,

$$H[P, R] = T[P] + V[R], \quad (1)$$

where *P* and *R* are the sets of nuclear momenta and positions. $T[P]$ is the nuclear kinetic energy,

$$T[P] = \sum_i \frac{P_i^2}{2M_i}, \quad (2)$$

where P_i is the momentum of the *i*-th nucleus and M_i is its mass. $V[R]$ is the nuclear potential energy

$$V[R] = E[R] + V_{NN}[R], \quad (3)$$

where $E[R]$ is the electronic ground state energy and $V_{NN}[R]$ the internuclear interaction energy for configuration *R*.

Let R_0 be a set of positions corresponding to a local minimum of the energy that we choose as a reference (e.g. the low-pressure phase *C*). Suppose that *R* differs from R_0 through the uniform strain tensor ϵ and the nuclear displacements u' :

$$R = R_0 \cdot (1 + \epsilon) + u', \quad (4)$$

where all site, vector, and tensor indices are understood, and the dot product implies a sum over all relevant site and component indices. Expanding V to second degree in ϵ and u' , we get:

$$V[R] = V[R_0] + \frac{1}{2} u' \cdot \frac{\partial^2 V[R_0]}{\partial u' \partial u'} \cdot u' + u' \cdot \frac{\partial^2 V[R_0]}{\partial u' \partial \epsilon} \cdot \epsilon + \frac{1}{2} \epsilon \cdot \frac{\partial^2 V[R_0]}{\partial \epsilon \partial \epsilon} \cdot \epsilon. \quad (5)$$

Making the substitution $u' = u + u_0$ with

$$u_0 = - \left(\frac{\partial^2 V}{\partial u' \partial u'} \right)^{-1} \cdot \frac{\partial^2 V}{\partial u' \partial \epsilon} \cdot \epsilon, \quad (6)$$

we obtain

$$H = T + \frac{1}{2} u \cdot \frac{\partial^2 V}{\partial u' \partial u'} \cdot u + \frac{1}{2} \epsilon \cdot \mathbf{C} \cdot \epsilon, \quad (7)$$

where

$$\mathbf{C} = \frac{\partial^2 V}{\partial \epsilon \partial \epsilon} - \frac{\partial^2 V}{\partial \epsilon \partial u'} \cdot \left(\frac{\partial^2 V}{\partial u' \partial u'} \right)^{-1} \cdot \frac{\partial^2 V}{\partial u' \partial \epsilon}. \quad (8)$$

Thus, when $\partial^2 V / \partial u' \partial u'$ becomes soft, that is, when it has eigenvalues which are nearly zero, \mathbf{C} will also become soft according to Eq.(8), provided the corresponding eigenfunctions of $\partial^2 V / \partial u' \partial u'$ couple to ϵ . In materials exhibiting PA, the modes which soften under pressure will couple to strains associated with elastic moduli that likewise soften under pressure.⁹ We can thus focus primarily on the softening of $\partial^2 V / \partial u' \partial u'$ and treat the strains implicitly, recognizing that the *u* in Eq.(7) contains them.

The transformation

$$X_{k\lambda} = \sum_{l\alpha} \exp(ikR_l) S_{\lambda\alpha}(k) u_{l\alpha} \quad (9)$$

diagonalizes H . In Eq.(9), the site index of Eq.(2) has been decomposed into a unit cell index *l*, with R_l the center of the *l*-th cell, and an internal index α . λ is the branch index of the normal mode $k\lambda$, *k* its wave vector in the first Brillouin zone, and $S_{\lambda\alpha}(k)$ is a unitary matrix for each *k*. The squares of the corresponding normal-mode frequencies $\omega_{k\lambda}$ are eigenvalues of the dynamical matrix $M^{-1/2} \cdot \partial^2 V / \partial u' \partial u' \cdot M^{-1/2}$. Thus if $\omega_{k\lambda}$ has a soft, flat branch in which $\omega_{k\lambda} \rightarrow 0$ for much of the

Brillouin zone, so does $\partial^2 V / \partial u' \partial u'$, as the mass matrix M is positive definite. Besides that of α -quartz under compression, there are other known examples of soft, flat branches. In the perovskite ferroelectrics, for example, there are optical branches which are unstable in the high-symmetry cubic structure, which, in that case, result in a ferroelectric phase transition.²⁵

We suppose that the subset $\{\mu\}$ of the set $\{\lambda\}$ of all branches are soft and flat. We construct their associated lattice Wannier functions²⁶ from the corresponding normal modes via the transformation

$$\begin{aligned} Y_{l\beta} &= \frac{1}{N} \sum_{k\lambda \in \{\mu\}} A_{\beta\lambda}(k) \exp(-ikR_l) X_{k\lambda} \\ &= \sum_{m\alpha} S_{l\beta,m\alpha} u_{m\alpha}. \end{aligned} \quad (10)$$

Since the $S_{l\beta,m\alpha}$ decay exponentially in $|R_m - R_l|$, the $Y_{l\beta}$ are local modes, optimally localized by proper choice of the phases and amplitudes of the unitary matrix elements $A_{\beta\lambda}(k)$; the flatter the branches $\{\mu\}$, the more localized. In the Einstein limit of zero dispersion, the $Y_{l\beta}$ are confined to a single cell. Also, the Hamiltonian contains no harmonic coupling between $Y_{l\beta}$ and $X_{k\lambda'}$ for those λ' not contained in $\{\mu\}$. These local modes form a basis for the construction of an effective Hamiltonian²⁶ much easier to use for simulations^{27,28} and, in our case, much easier to model than the original Hamiltonian.

IV. THE MODEL HAMILTONIAN

Ignoring the uniform strain ϵ , the Hamiltonian in Eq. (1) can be decomposed into contributions from the soft flat branches $\{\mu\}$, the remaining branches $\{\mu'\}$, and their interaction arising from anharmonicity in $V[R]$:

$$H = H_{\{\mu\}} + H_{\{\mu'\}} + H_{\{\mu\}\{\mu'\}}. \quad (11)$$

In developing the model Hamiltonian, only the contribution of the soft, flat branches, $H_{\{\mu\}}$, is considered explicitly. $H_{\{\mu'\}}$ is replaced implicitly by the Hamiltonian of a thermal reservoir at temperature T and $H_{\{\mu\}\{\mu'\}}$ is replaced by an appropriate coupling of the $\{\mu\}$ to the reservoir.

In what follows we drop the subscript $\{\mu\}$ from $H_{\{\mu\}}$. The dependence of the potential V on the local mode amplitudes $Y_{l\beta}$ can be expressed as a cluster expansion so that H takes the form

$$\begin{aligned} H &= \sum_{l\beta} \frac{P_{l\beta}^2}{2M_\beta} + \sum_l V_l(Y_{l\beta}) + \sum_{l \neq m} V_{lm}(Y_{l\beta}, Y_{m\beta'}) \\ &+ \sum_{l \neq m \neq n} V_{lmn}(Y_{l\beta}, Y_{m\beta'}, Y_{n\beta''}) + \mathcal{O}(Y^4), \end{aligned} \quad (12)$$

where $\beta, \beta', \beta'', \dots \in \{\mu\}$. We now assume all essential physics remains if we limit the anharmonicity to the local

term $V_l(Y_{l\beta})$, a restriction which simplifies H to

$$\begin{aligned} H &= \sum_{l\beta} \frac{P_{l\beta}^2}{2M_\beta} + \sum_l V_l(Y_{l\beta}) \\ &+ \frac{1}{2} \sum_{l \neq m} V_{lm}^{\beta\beta'}(Y_{l\beta} - Y_{m\beta})(Y_{l\beta'} - Y_{m\beta'}). \end{aligned} \quad (13)$$

If we now suppose that only a single branch becomes soft and flat, H further simplifies, after dropping the index β , to

$$H = \sum_l \frac{P_l^2}{2M} + \sum_l V_l(Y_l) + \frac{1}{2} \sum_{l \neq m} V_{lm}(Y_l - Y_m)^2. \quad (14)$$

As described in the Sec. II, we are dealing with strongly first-order phase transitions. The simplest functional dependence of $V_l(Y_l)$ which can lead to such phase transitions is that of a sixth degree polynomial,

$$V_l = \frac{1}{2}AY_l^2 - \frac{1}{4}BY_l^4 + \frac{1}{6}CY_l^6, \quad (15)$$

where B and C are positive, and A can be positive or negative. Not enough is gained by including coefficients V_{lm} beyond nearest neighbors to warrant the added complexity and increase in the number of parameters. The harmonic coupling term is then taken to be simply $\frac{1}{2}V_1 \sum_{\langle l,m \rangle} (Y_l - Y_m)^2$, where the notation $\langle l,m \rangle$ implies that the sum is restricted to nearest-neighbors only.

We now scale displacement by the factor $L = \sqrt{B/C}$, time by $t_0 = B^2/MC$, momentum by ML/t_0 , and energy by B^3/C^2 . The resulting scaled Hamiltonian has the form

$$H = \sum_l \frac{1}{2}P_l^2 + \sum_l V_{\text{loc}}(u_l) + \frac{1}{2}k \sum_{\langle l,m \rangle} (u_l - u_m)^2, \quad (16)$$

where H is the scaled Hamiltonian and P_l and u_l are the scaled local-mode momenta and amplitudes. $V_{\text{loc}}(u_l)$ takes the form

$$V_{\text{loc}}(u_l) = \frac{1}{2}\alpha u_l^2 - \frac{1}{4}u_l^4 + \frac{1}{6}u_l^6, \quad (17)$$

where

$$\alpha = \frac{AC}{B^2}, \quad (18)$$

and k in Eq. (16) is

$$k = \frac{V_1 C}{B^2}. \quad (19)$$

For definiteness we take V_1 , and therefore k , to be positive. H thus depends only on the two parameters α and k . We take it to be classical.

The local mode amplitudes u_l evolve with time under the influence of H and the coupling to the reservoir. We

presume u_l to follow Langevin dynamics with the equation of motion

$$\ddot{u}_l = -\frac{\partial V_{\text{tot}}}{\partial u_l} - \frac{1}{\tau}\dot{u}_l + F_l, \quad (20)$$

where

$$V_{\text{tot}} = \sum_m V_{\text{loc}}(u_m) + \frac{1}{2}k \sum_{\langle m,n \rangle} (u_m - u_n)^2 \quad (21)$$

is the total potential. F_l is a Gaussian random force exerted by the reservoir with moments

$$\langle F_l(t) \rangle = 0, \text{ and} \quad (22)$$

$$\langle F_l(t)F_m(t') \rangle = \mathcal{F}\delta_{lm}\delta(t-t'). \quad (23)$$

Equipartition requires that

$$\langle \dot{u}_l^2 \rangle = \frac{1}{2}k_B T \quad (24)$$

with T the reservoir temperature. The fluctuation-dissipation theorem requires that

$$\frac{1}{\tau} = \frac{\mathcal{F}}{k_B T}. \quad (25)$$

Thus we are faced with a four-parameter problem (α, k, τ, T) even with this simplest of models. Achieving a detailed understanding of the physics of the model requires extensive numerical simulation. However, many of its important qualitative features are readily extracted, yielding important insights into the nature of pressure amorphization in those materials to which the model might be relevant, as described in the next four sections. The results of the simulations will be reported separately.²⁹

V. PRESSURE AMORPHIZATION

We now proceed to elucidate the potential energy landscape of our model. For $\alpha > 3/16$ and $\forall k$ in Eq.(21), V_{tot} has a global minimum at $u_l = 0$, $\forall l$, at which $V_{\text{tot}} = 0$. We assign this minimum to the low-pressure crystal structure C described in Sec. II. When $\alpha < 3/16$ and $\forall k$, there are two equivalent global minima with

$$u_l = w = \left[\frac{1}{2} + \sqrt{\frac{1}{4} - \alpha} \right], \forall l, \text{ and} \quad (26)$$

$$u_l = -w = -\left[\frac{1}{2} + \sqrt{\frac{1}{4} - \alpha} \right], \forall l \quad (27)$$

at which

$$V_{\text{tot}} = \frac{1}{3}N\left[\frac{3}{4}\alpha - \frac{1}{8} - \left(\frac{1}{4} - \alpha\right)^{3/2}\right] < 0. \quad (28)$$

We take this structure to represent the high-pressure crystal structure C' of Sec. II. Thus, there is a first-order

phase transition at $\alpha = 3/16$ from C to C' as α decreases monotonically with pressure p irrespective of the value of k . The two spinodals occur at $\alpha = 1/4$ and $\alpha = 0$, $\forall k$. For the phase transition $C \leftrightarrow C'$ to be strongly first-order in the sense used in Sec. II., a variation in α from $1/4$ to 0 can be thought of as occurring via substantial change of pressure. The barrier between C and C' at the transition (where $\alpha = 3/16$) is $1/96$, so that the reduced temperature T must be taken substantially lower than $1/96$ for strong hysteresis to occur, as it does in type I materials.

We first consider the Einstein case in which $k = 0$. For $3/16 < \alpha < 1/4$, 2^N degenerate local minima exist in V_{tot} with energy given by Eq.(28), except that V_{tot} is positive in this range. The magnitude of u_l is given by w in Eq.(26), its sign being arbitrary. As α falls below $3/16$, all 2^N phases become equivalently stable relative to C . Among these 2^N phases, two correspond to *single-crystal* C' , and an exponentially small fraction to *poly-* or *micro-crystalline* C' ; yet the vast majority of the structures are *amorphous* in that there is at most short-range order in the u_l even though a clear topological memory of the original crystal structure C remains. Barriers keep the system in C until the spinodal at $\alpha = 0$ is approached. At the spinodal, C becomes locally unstable relative to all 2^N phases. The probability of the system finding its way from C to one of the amorphous phases is vastly higher than that to one of the exponentially fewer polycrystalline C' phases.

More generally, pressure amorphization occurs if (i) there is a region of the α - k plane in which the a phases are more stable than the C phase but metastable with respect to C' and (ii) if τ and T are such that a is preferentially accessible from C either irreversibly (types I, II, and IV) or temporarily (types III and V). In the next three sections we shall argue that this indeed holds for the 2-site case, the 3-site case, and the N -site case by examining the topology of the potential-energy landscape presented by $V[u]$. In reading these sections, it is important to bear in mind that k determines how flat the branch is and α how soft. A soft, flat branch has small α and small k .

Note that the previous discussion straightforwardly applies to the case in which there are ν flat branches. $V[Y]$ is then defined on a νN -dimensional configuration space. Around every minimum in this space there is a basin of attraction bounded by a separatrix, a hypersurface of dimension $\nu N - 1$. As in the single-branch case, PA will occur when the amorphous minima a are preferentially accessible from C .

VI. THE 2-SITE MODEL

To begin, we study pressure amorphization in our simple Hamiltonian through analysis of the topology and kinetics of a 2-site model. In what follows the local-mode amplitude and momentum of the first site are x and P_x ,

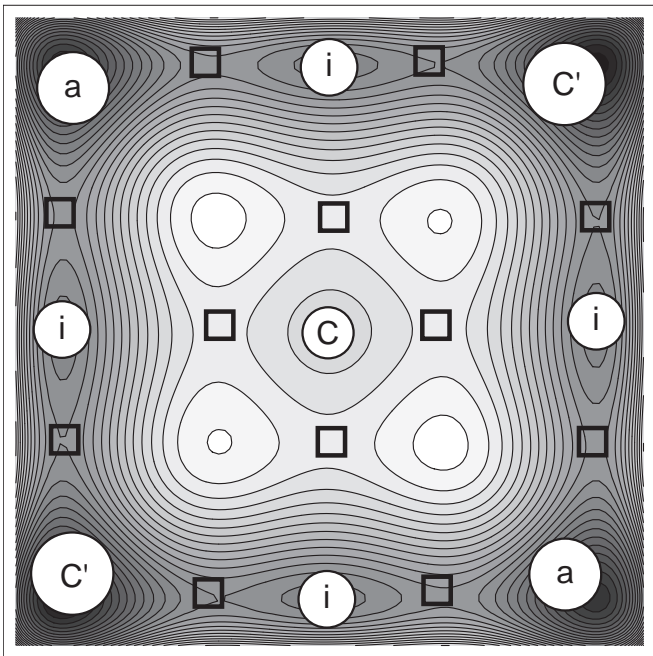


FIG. 1: Contour plot of the potential $V(x, y)$ of the 2-site model in the xy plane. Minima are indicated by white circles and saddle points by open squares; the maxima are clear by inspection. The larger the symbol, the lower the value of $V(x, y)$. The crystalline minima are indicated by C or C' , the intermediate minima by i , and the amorphous minima by a .

those of the second site y and P_y . The Hamiltonian is

$$H = T + V, \quad (29)$$

where

$$T = \frac{1}{2}(P_x^2 + P_y^2) \quad (30)$$

and

$$V = \frac{1}{2}\alpha(x^2 + y^2) - \frac{1}{4}(x^4 + y^4) + \frac{1}{6}(x^6 + y^6) + \frac{1}{2}k(x - y)^2. \quad (31)$$

In Fig. 1, we show in the xy configuration plane the critical points of $V(x, y)$ for $k = 0$ and $0 < \alpha < 3/16$. C occurs at $x = y = 0$, C' at $x = y = \pm w$. There is only one saddle point separating the C , C' , or a basins from each neighboring intermediate i basin.

In Fig. 2, we divide the α - k phase plane into regions each of which has a distinct critical point (CP) structure, labelling each region (with one exception) by the stable crystal structure within it and displaying the CP structure. The exception, shaded, is the region within which V retains at finite k for $0 < \alpha < 3/16$ the same topology, i.e. CP structure, that it has for $k = 0$ as shown in Fig. 1. It is only within this region that PA is possible because the a minima exist, they are stable relative to C ,

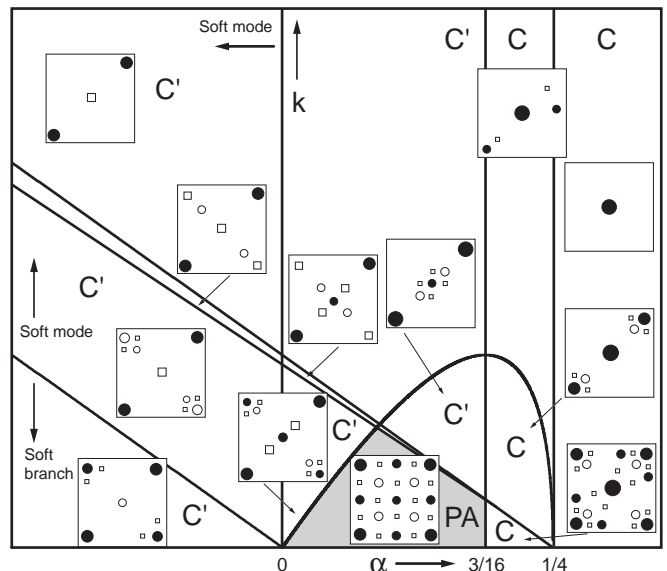


FIG. 2: The α - k phase plane of the 2-site model divided into regions of distinct critical point structure. Maxima are indicated by open circles, minima by solid circles, and saddle points by open squares. The sizes of the circles reflect the relative magnitudes of the extrema. Each region is labelled by the stable crystal structure within it, except for one. Within that region, marked PA, the critical point structure is the same as for $k = 0$, $0 < \alpha < 3/16$, and pressure amorphization is possible as discussed in the text.

and both a and C' can be reached from C only by trajectories which must pass through intermediate basins i so that the transition C to a can compete kinetically with C to C' .

For PA to occur within this 2-site model, trajectories from C to a must be traversed with some probability relative to those from C to C' . This happens if the following seven conditions are met:³⁰ (i) The minimum must exist and be stable relative to C ; (ii) Intermediate basins of attraction must exist, and all statistically significant trajectories from C to C' or a must pass through them; (iii) For hysteresis, both $V_{ic} - V_c$ and $V_{ia} - V_a$ must be much larger than $k_B T$ at $\alpha = 3/16$; (iv) For ia to be accessible from ic , one requires $V_{ic} - V_{ia} \gtrsim 0$ and slow relaxation in the i basin; (v) For the probabilities of transitions from i to a and from i to C' to be of comparable magnitudes, $V_{ia} - V_{ic'}$ must not be much larger than $k_B T$; (vi) For the transition from i to a to be irreversible, or likewise for there to be a very long resident time in a before a transition from a to C' , $V_{ia} - V_a \gg k_B T$ and fast relaxation must occur in the basin; (vii) Finally, for consistency of (v) and (vi), τ must not be too low. Detailed qualitative considerations strongly suggest that these conditions can be met only for α and k in the shaded region of Fig. 2, provided that the remaining parameters T and τ assume appropriate values. The actual determination of the probability of $C \rightarrow a$ relative to that for $C \rightarrow C'$ for

various values of T and τ requires numerical simulation, the results of which will be reported elsewhere.

We have supposed that α is a monotonically decreasing function of pressure. For simplicity, we shall further suppose that k depends weakly on p as α decreases. The effect of pressure change on the system can be represented by a trajectory in the α - k plane. One can readily see that the five types of behavior described in Sec. II have direct parallels in the responses of our model system along different trajectories in the α - k plane. For example, a trajectory which starts at $\alpha > 1/4$ and moves well into the PA region before reversing and returning corresponds to type I behavior, with p_{ca} corresponding to $0 < \alpha_{ca} < 3/16$ and p_{ac} corresponding to $3/16 < \alpha_{ac} < 1/4$. Type II corresponds to a trajectory that starts in structure C at $\alpha = \alpha_0$ with $3/16 < \alpha_0 < 1/4$, transforms into a below $0 < \alpha_{ac} < 3/16$, and can return to α_0 while still being amorphous. Trajectories terminating in the PA region near its upper right boundary correspond to behavior typical of type III materials. A trajectory which starts at $\alpha > 1/4$ and passes through the PA region into that with $\alpha < 0$ would correspond to the situation in a type IV material. Finally, trajectories which, on their return to larger α , pass through the upper right boundary can undergo an $a \rightarrow C'$ transition inside the boundary, remaining in C' upon pressure reduction until some α in $(3/16, 1/4)$ is reached; these would correspond to transitions in type V materials.

VII. THE 3-SITE MODEL

We now discuss an extension of the model described in Sec. VI to three sites. We label the third site by z and suppose it is coupled only to y as in a linear triatomic molecule. An additional term $P_z^2/2$ is added to T in Eq.(30), and V becomes

$$V = \frac{1}{2}\alpha(x^2 + y^2 + z^2) - \frac{1}{4}(x^4 + y^4 + z^4) + \frac{1}{6}(x^6 + y^6 + z^6) + \frac{1}{2}k[(x-y)^2 + (y-z)^2]. \quad (32)$$

Just as in the 2-site model, there is a region in the α - k plane within which the CP structure and the topology of V remain the same as for $k = 0$. It is within this region that PA can occur. Its shape is qualitatively the same as that for the 2-site model, bounded by the α -axis from 0 to $3/16$ and on the right by a vertical segment at $\alpha = 3/16$. The upper boundary segments, however, are displaced towards smaller k .

The $k = 0$ minima are shown in Fig. 3. For small but finite k in the PA region, the structure is compressed perpendicular to the $x = y$ and $y = z$ planes. There are now six classes of minima: one C , six i_1 , six i_2 , six i'_2 , six a , and two C' , using the notation of Fig. 3. The sequence of values of V at the minima is $V_C > V_{i_1} > V_{i'_2} > V_{i_2} > V_a > V_{C'}$. The sequence at the saddles is $V_{ci} > V_{i_1 i'_2} > V_{i_1 i_2} > V_{i_2 a}, V_{i'_2 a}, V_{i'_2 C'}$

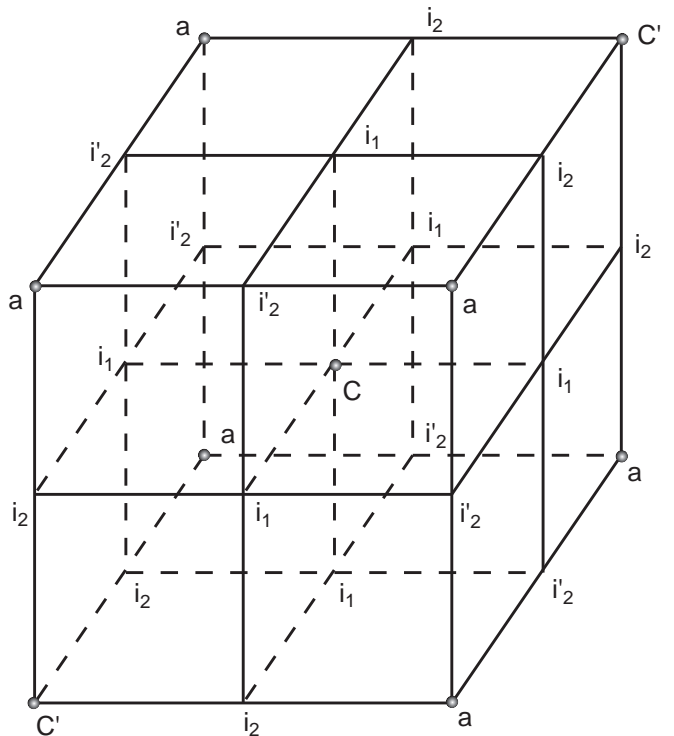


FIG. 3: Minima of the potential energy landscape of the 3-site model.

and $V_{ci} - V_{i_1 i'_2} \gg V_{i_1 i'_2} - V_{i_1 i_2}$, etc. These sequences have the following implications. As before, transitions between the basins occur over separatrices near the transition states (saddle points). Relaxation can be fast enough to bias the transformation down hill but still slow enough that enough energy remains to get over each successive barrier with little difference between rates over the primed and unprimed barriers. To reach C' from C , the system must follow the sequence $C \rightarrow i \rightarrow i_2 \rightarrow C'$ for which there are 12 independent routes. To reach a from C , the system can follow either of two sequences, $C \rightarrow i \rightarrow i_2 \rightarrow a$ or $C \rightarrow i \rightarrow i'_2 \rightarrow a$, for which there are 36 routes, or 3 times as many as for $C \rightarrow C'$. This increase in the number of paths from C to a relative to that from C to C' compensates for the more favorable kinetics of the final step from i_2 to C' , increasing the probability of $C \rightarrow a$ relative to that of $C \rightarrow C'$ over that of the two-site model.

VIII. THE N -SITE MODEL

We now jump to a model with a macroscopically large number of equivalent sites each of which is coupled to a finite number of nearest neighbors via the harmonic term in V . Once again, there is a domain in the α - k plane in which the topology of V is the same for finite k as for $k = 0$. Its lower boundary is unchanged at $k = 0$,

$0 < \alpha < 3/16$. Its upper boundary is further compressed, the degree of compression increasing with the number of nearest neighbors. Just as the minima for the 3-site case lie at the center, face centers, edge centers, and corners of a cube, so are the minima arranged on an N -dimensional hypercube in the N -dimensional configuration space for $k = 0$. As k increases, the CP structure distorts without change of topology up to some k which depends on α . The existence of this finite domain of topological stability is guaranteed by the analyticity of V , its gradient, and its Hessian in the configuration space. There is now one minimum of type C , $3^N - 2^N - 1$ of type i , $2^N - 2$ of type a , and 2 of type C' . The sequence of values of V is $V_c > V_i > V_a > V_{C'}$.³¹ The number of a minima is exponentially larger than the number of C' minima, even if one extracts the polycrystalline C' structures from the above number of a 's and adds them to the C' 's, as one can see from the following estimate. Let n be the minimum grain size. Then $2^{N/n}$ is a lower bound but still a good estimate of the number of polycrystalline structures. The corrected ratio of C' 's to a 's is thus estimated to be

$$\frac{2^{-N(1-1/n)}}{1 - 2^{-N(1-1/n)}} \xrightarrow{N \rightarrow \infty} 0, \text{ with } n > 1, \quad (33)$$

which is still exponentially small. The number of paths from C to a is correspondingly exponentially larger than that from C to C' , overcoming any kinetic advantage of any single path from C to C' . In conclusion, the key to PA within this model is the existence of a region of the α - k plane within which the $k = 0$ topology persists, a region of a flat (small k) and soft but not unstable ($0 < \alpha < 3/16$) branches together with τ and T in a suitable range.

IX. RELATION TO CONVENTIONAL NUCLEATION AND GROWTH MECHANISM

Suppose the transformation $C \rightarrow C'$ were to occur by the conventional nucleation and growth mechanism with \dot{I} the nucleation rate and \dot{R} the growth rate.³³ For \dot{I}/\dot{R} finite, a polycrystal of C' results. In the limit $\dot{I}/\dot{R} \rightarrow 0$, a single crystal results. In the limit $\dot{I}/\dot{R} \rightarrow \infty$, a nanocrystalline material results, and we can imagine that in the ultimate limit in which nucleation totally dominates growth, an amorphous phase results when the crystallite is so small that there is no distinction between bulk and grain boundary. In the classical theory of nucleation, the critical radius of the nucleus of C' is

$$R^* = \frac{2\sigma}{\Delta g}. \quad (34)$$

Here Δg is the bulk Gibbs free-energy difference between C and C' , and σ is the interfacial free energy. The corresponding barrier to nucleation is

$$\Delta G^* = \frac{16\pi}{3} \frac{\sigma^3}{(\Delta g)^2}. \quad (35)$$

For nucleation completely to dominate growth and for the critical size nucleus to be so small that the result is an amorphous phase, it is obvious from Eqs. (34) and (35) that σ must become small. σ measures the free-energy cost of a rapid local structural change from C to C' . In our simple model, the energy cost of such a structural change is simply proportional to the coupling constant k . Thus, our finding the possibility of pressure amorphization in the region of the α - k plane within which the $k = 0$ topology of V is preserved is completely consistent with nucleation theory, the smallness of k corresponding to small σ and the existence of intermediate minima corresponding to finite Δg and slow growth rate. To conclude, PA occurs when nucleation totally dominates growth.

X. SUMMARY AND CONCLUSIONS

In this work, we make a clear distinction between two types of amorphous phases. The first, the conventional glassy phase, is not topologically equivalent to any crystalline phase, and glass formation from the crystal is a reconstructive transformation.³³ Such glasses are formed, for example, by sufficiently rapid cooling from the melt. A conventional glass can form via pressure amorphization if (i) the limit of local stability of C relative to its melt (the spinodal) is approached, and (ii) if the glass transition temperature of the melt is then higher than the equilibrium melting temperature of C .^{3,4} Here we are concerned not with conventional glasses, but with pressure-induced amorphous phases in which the structural instability that leads to the amorphization is associated with one or more soft, flat branches of the phonon spectrum and in which memory of the original topology of the low-pressure crystal structure is retained through the remaining stable branches. In such cases, the amorphization arises from a random displacive or orientational transition instead of from a reconstructive transition.

This type of pressure amorphization is driven by an underlying strongly first-order structural phase transition $C \rightarrow C'$ under compression. In our view, as C becomes thermodynamically unstable relative to C' , there is one or more branches which flatten with increasing pressure. Local modes in the form of lattice Wannier functions provide a natural means of description of such flat branches. We have supposed that the nonlinearities associated with the first-order phase transition arise primarily in the amplitudes of the individual local modes, an inessential simplification. We have argued that there is a range of pressures within which the local nonlinearities and relative flatness of the relevant branch or branches allow an exponentially large number of amorphous structures to be metastable and preferentially kinetically accessible over C relative to the thermodynamically stable single crystal or polycrystalline C' phase. Such metastability and kinetic preference occur within a restricted region of the parameter space defining the potential energy landscape in the configuration space of the local modes,

as shown explicitly for the 2-site model in Fig. 2. The ambient temperature must be low enough to lead to substantial hysteresis ($T \ll 1/96$), so that C persists well into its domain of metastability as p increases. Once the structural transition is initiated, it proceeds downhill via an exponentially large number of paths through the basins of attraction of intermediate structures without being trapped there, requiring relaxation rates in a suitable range. If trapping were to occur, it would correspond to intermixed amorphous a , intermediate, and crystalline C regions, resulting in observable Bragg peaks associated with C . Further compression (i.e., further reduction of α) would result in a drop in the fraction of C , decreasing Bragg peak intensities. That is, trapping implies a broadened C to a transition. The intermediate basins correspond to a random admixture of both C -like and C' -like local configurations.

Normally, first-order structural transitions are discussed in terms of nucleation and growth. In the present picture, the critical size nucleus is not much more than a single unit cell (with minor displacements in neighboring cells) and nucleation overwhelms growth, leaving the system in an amorphous structure when nucleation is complete.

The type of pattern observed in the structural transitions caused by pressure changes depends on the partic-

ular trajectory through the parameter space of the potential which is induced by the changing pressure.

The picture developed in this paper can embrace all of the phenomena which have been observed in association with pressure amorphization. Nevertheless, the discussion has been largely qualitative. Obtaining a quantitative demonstration that these simple models admit pressure amorphization requires numerical simulation.²⁹ Once that has been demonstrated, such simulations should be carried out for real materials since substantial experience has already been built up in constructing effective Hamiltonians of the type considered here for specific substances.^{26,27,28} Among the tasks for simulations is to distinguish whether the occurrence of pressure amorphization results in a conventional glass or leaves the crystalline topology invariant for a particular material.

Acknowledgments

We greatly benefitted from discussions with A. Angel, R. Car, J. R. Chelikowsky, P. Giannozzi, G. N. Greaves, G. S. Grest, K. M. Rabe, S. Scandolo, and D. Vanderbilt. J. I. acknowledges the financial support of the ONR through Grant N0014-97-1-0048.

-
- ¹ L. H. Brixner, *Mater. Res. Bull.* 7 (1972) 879.
² O. Mishima, L. D. Calvert, and E. Whalley, *Nature* 314 (1985) 76.
³ E. G. Ponyatovsky and O. I. Barkalov, *Mater. Sci. Rep.* 8 (1992) 147.
⁴ F. Sciortino *et al.*, *Phys. Rev. E* 52 (1995) 6484.
⁵ S. M. Sharma and S. K. Sikka, *Prog. Mater. Sci.* 40 (1996) 1.
⁶ P. Richet and P. Gillet, *Eur. J. Mineral.* 9 (1997) 908.
⁷ G. N. Greaves, NATO Advanced Research Workshop "Frontiers of High Pressure Research III: Application of High Pressure to Low Dimensional Electronic Materials", Colorado State University, 2001, Kluwer Academic (in press).
⁸ J. S. Tse and D. D. Klug, *Phys. Rev. Lett.* 67 (1991) 3559.
⁹ N. Binggeli and J. R. Chelikowsky, *Phys. Rev. Lett.* 69 (1992) 2220.
¹⁰ S. L. Chaplot and S. K. Sikka, *Phys. Rev. B* 47 (1993) 5710.
¹¹ M. S. Somayazulu, S. M. Sharma, and S. K. Sikka, *Phys. Rev. Lett.* 73 (1994) 98.
¹² N. Binggeli, N. Keskar, and J. R. Chelikowsky, *Phys. Rev. B* 49 (1994) 3075.
¹³ G. W. Watson and S. C. Parker, *Phys. Rev. B* 52 (1995) 13306.
¹⁴ J. S. Tse, D. D. King, Y. Le Page, and M. Bernasconi, *Phys. Rev. B* 56 (1997) 10878.
¹⁵ S. Baroni and P. Giannozzi, *High Pressure Materials Research*, eds. R. M. Wentzcovitch *et al.*, *Mat. Res. Soc. Symp. Proc.* 499 (1998) 233.
¹⁶ R. W. Wentzcovitch, C. da Silva, and J. R. Chelikowsky, *Phys. Rev. Lett.* 80 (1998) 2149.
¹⁷ D. W. Dean, R. M. Wentzcovitch, N. Keskar, J. R. Chelikowsky, and N. Binggeli, *Phys. Rev. B* 61 (2000) 3303.
¹⁸ J. S. Tse and D. D. Klug, *Science* 255 (1992) 1559.
¹⁹ N. R. Keskar, J. R. Chelikowsky, and R. M. Wentzcovitch, *Phys. Rev. B* 50 (1994) 9072.
²⁰ L. E. McNeil and M. Grimsditch, *Phys. Rev. Lett.* 68 (1992) 83.
²¹ J. S. Tse and D. D. Klug, *Phys. Rev. Lett.* 70 (1993) 174.
²² G. Richard and P. Richet, *Geophys. Res. Lett.* 17 (1990) 2093.
²³ Q. Williams *et al.*, *J. Geophys. Res.* 95 (1990) 21549.
²⁴ M. B. Kruger, *et al.*, *Science* 255 (1992) 703.
²⁵ Ph. Ghosez, E. Cockayne, U. V. Waghmare and K. M. Rabe *Phys. Rev. B* 60 (1999) 836.
²⁶ K. M. Rabe and U. V. Waghmare, *Phys. Rev. B* 52 (1995) 13236.
²⁷ U. V. Waghmare and K. M. Rabe, *Phys. Rev. B* 55 (1997) 6161.
²⁸ W. Zhong, D. Vanderbilt, and K. M. Rabe, *Phys. Rev. Lett.* 73 (1994) 1861; *ibid.*, *Phys. Rev. B* 52 (1995) 6301; J. Íñiguez *et al.*, *Phys. Rev. B* 63 (2001) 144103.
²⁹ J. Íñiguez, M. H. Cohen, and J. B. Neaton, to be published.
³⁰ In the following, single subscripts on V indicate the value of V at a minimum. Double subscripts indicate its value at a saddle point lying on the separatrix between the two minima specified by the subscript.
³¹ Both V_i and V_a have a range $O(N)$.
³² D. Turnbull and J. C. Fisher, *J. Chem. Phys.* 17 (1949) 71.
³³ D. Turnbull and M. H. Cohen, *J. Chem. Phys.* 29 (1958) 1049.